

# Asymmetrical Heat Transfer Intensification Method for High-Temperature Gas Turbines Blades

I.V. Shevchenko, A.N. Rogalev<sup>1</sup>, I.V. Garanin, I.I. Komarov and A.N. Vejera

National Research University "Moscow Power Engineering Institute",  
Krasnokazarmennaya str. 14, 111250, Moscow, Russian Federation

Orcid ID:<sup>1</sup> 0000-0001-7256-0144

## Abstract

External flow around the profile of the gas turbine blade produces a non-uniformity in the values of the heat transfer coefficient along the contour of the profile and differences between the pressure and suction sides. To equalize the temperature field, the cooling system of the blade must be designed to provide more intensive heat exchange in thermal stressed locations. As well as in some cases additional intensification is required only at pressure or suction side. Both of these aspects are critical to ensuring the necessary mechanical reliability of the gas turbine blades.

Paper presents the results of a numerical and experimental study of an new heat transfer augmentation system in radial channels developed for alignment of the temperature field from the suction and pressure sides. A CFD simulation for a wide range of Reynolds numbers was carried out using ANSYS CFX software. Effect of model geometrical parameters on the heat transfer distribution asymmetry was determined. Presented a results of blade with the proposed intensification system tests conducted in a liquid-metal thermostat.

**Keywords:** Turbine blade, cooling channels, heat transfer augmentation, intensification coefficient, temperature field irregularity.

## INTRODUCTION

The serpentine-like one and half-pass cooling channel systems are broadly used in cooling of the gas turbine blades. The median section of these blades has the radial channels with the centrifugal and radial-inward cooling air flow. The heat transfer turbulators in a form of the cross-sectional or angled ribs [1, 2, 3, 4] used in channels of the feather median sections failed to eliminate the temperature irregularity from the suction and pressure sides, which is reaching 200°C for a first stage blade of the high-pressure turbine for an aircraft engine. This irregularity derived from distribution of gas velocities in the cascade blade channel, while in blade systems with a low-aspect ratio it is derived from the effect of a vortex pair from the suction side [5, 6]. Difference in temperature of the suction and pressure sides causes additional thermal stresses and, as a

result, decreasing of blade strength coefficients. A film cooling with supply of the cooling air to the feather external surface through several perforation rows is used to reduce the temperature from the pressure side.

The structural drawing of the turbine blade for an aircraft engine with the combined convective and film cooling is given in Fig. 1 as an example of such structural design. Maximum gas temperature gas max is equal to 1700 K [7] and relative flow rate of cooling air  $G_{cool,air}$  is equal to 4.3%. Three rows of perforation holes having diameter of 0.35 mm and inclined to the blade peripherals at an angle of 45° are installed on the blade leading edge. Three perforation rows are made on the blade concave side having the first row diameters of 0.35 mm and diameters of two following rows – 0.47 mm.

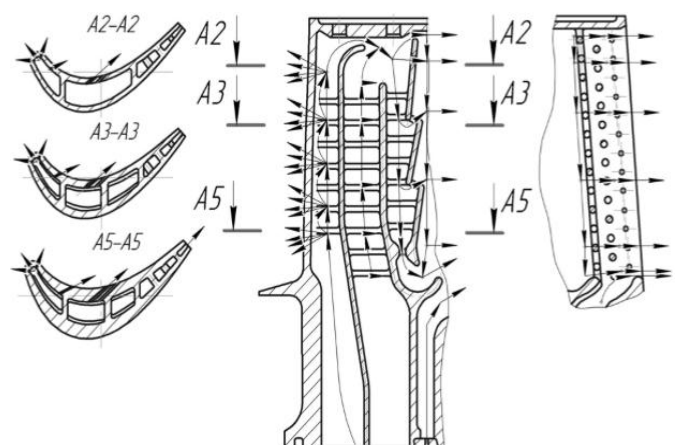


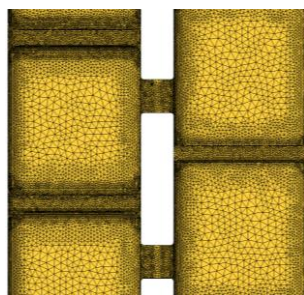
**Figure 1:** Structural design of the rotor blade for HPT with the film cooling

The average value of a blade relative cooling depth is  $\theta_{av} = 0.43$ . This value is close to the cooling rate of the blade with a convective cooling, but with relation to a decrease in temperature gradients across the blade feather, in other words a difference in temperatures between the pressure and suction sides, it has obviously an essential advantage. However, a relative flow rate of the cooling air for cooling the blade median section is higher by 22%.

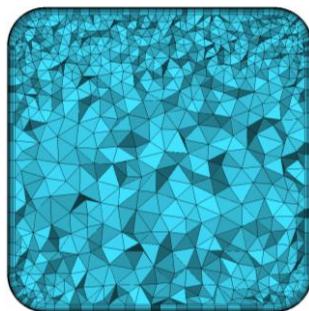
Research and development of asymmetrical heat transfer augmentation methods in radial cooling channels of turbine blades allowing to reduce the irregularity of temperature field in a feather cross section without the use of film cooling was the purpose of this article.

### CFD METHOD

Software tool ANSYS CFX was used for simulation of heat-mass exchange processes in cooling channels. Set of Reynolds-averaged Navier-Stokes equations (RANS equations) using  $k-\omega$  turbulence model with an automatic wall function was solved in this software module. This setup is often used in same type of flow [8, 9]. A computational grid was drawn in ICEM program. Interior grid: unstructured, tetrahedral with prismatic layer. Maximum linear dimension is 0.0025 m. Minimal linear dimension of grid elements is 0.0005 m. A near-wall region has detailed resolution using the prisms with the following parameters: number of layers – 11, prism initial height – 0.000002 m, growth law – WB-exponential. Total element number – 20-30 mln. Mesh general view shown in Fig. 2.



a)



b)

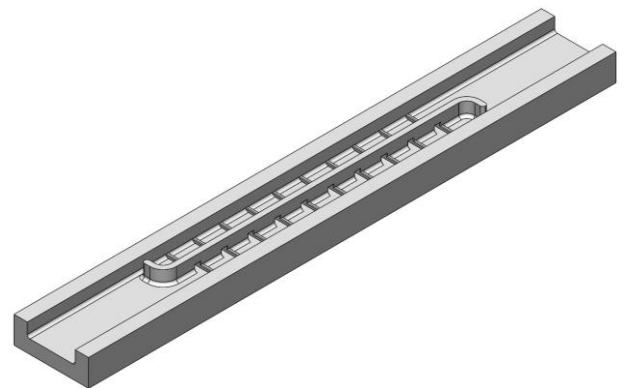
a) – in the proximity of holes; b) – cross section

**Figure 2:** Computational grid

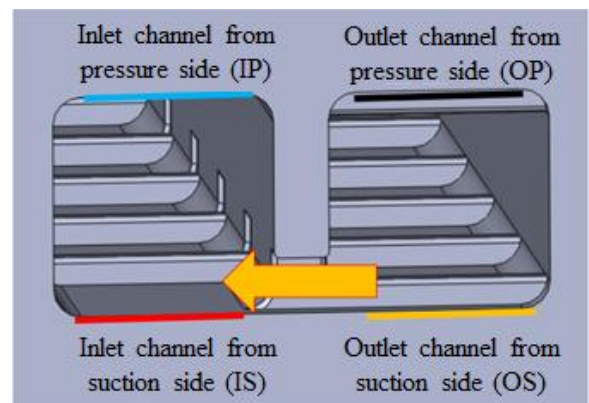
### MODELS DESCRIPTION

Model of the feather median section consisting of two square cross section channels (4 x 4 mm) was the object of research. The channel walls had a cross-sectional ribbing. Ribs were installed at an angle of 90° to the air flow direction. Rib height

is 0.5 mm, width – 0.5 mm, pitch – 5 mm. On the opposite walls the ribs were offsetted by half a pitch. A general view of the model is shown in Fig. 3



a)



b)

a) – view of model with removed wall; b) – model cross section

**Figure 3:** Model studied

The inlet channel, located on the right side, is connected with the outlet channel through the holes made in a separation rib on the wall simulating the pressure side. Ribs in the inlet channel are installed downstream of the holes and in the outlet channel – upstream of the holes. The hole height was equal to the rib height of 0.5 mm, hole length was set at 0.5, 1.0 and 1.5 mm. The separation rib had a bend on its ends for simulation of the open flow area restriction at the inlet of outlet channel and at the outlet of inlet channel.

First kind boundary conditions were set on the channel external surface – wall temperature was 419°C, air temperature at the model inlet was 20°C, range of Reynolds numbers – from 6000 to 55000. Thermal conductivity of the model walls – 16 W/m·K. Ten cases of the channels were studied; their geometric parameters are given in Table 1. The inlet and outlet channel restrictions for each case were equal. Case 1 (two parallel channels without restrictions and with two-side ribbing) was taken as a basic case.

**Table 1:** Model geometric dimensions

Case	Hole, mm	Hole area, mm <sup>2</sup>	Restriction, mm	Restriction area, mm <sup>2</sup>
1 (basic)	0	0	4	16
2	1	1	1	4
3	1	1	2	8
4	1	1	3	12
5	0.5	0.5	1	4
6	0.5	0.5	2	8
7	0.5	0.5	3	12
8	1.5	1.5	1	4
9	1.5	1.5	2	8
10	1.5	1.5	3	12

## RESULTS AND DISCUSSIONS

The distribution of local heat transfer coefficients lengthwise of the channels from the suction and pressure sides, values of Nusselt numbers  $Nu$ , relative Nusselt numbers (intensification coefficient)  $K = Nu/Nu_0$  were determined based on the performed calculation data.  $Nu_0$  was calculated by the equation (1).

$$Nu_0 = 0.021 \cdot Re^{0.8} \cdot Pr^{0.43}, \quad (1)$$

where  $Re$  – Reynolds number;

$Pr$  – Prandtl number.

Relative coefficient of linear hydraulic resistance determined as:  $f/f_0$ . Base hydraulic resistance  $f_0$  was calculated with Blasius equation.

$Nu/Nu_0$  and  $f/f_0$  values averaged lengthwise of the channels were also determined on the basis of which a preliminary data analysis was performed in Tables 2 and 3.  $K$  values for  $Re \approx 20000$  in channels are given in Table 4.

Cases 5 and 6 (Table 2) are most preferred as compared to the case 1. They ensure retention of the intensification level from the suction side and it's increasing from the pressure side. If  $K$  relation from the suction and pressure sides (Table 4) will be used as a criterion, than in this case reference should be made to the cases with a larger hole area (cases 2, 3, 4 and 8, 9, 10).

A heat transfer augmentation rate depends on the hole dimensions and channel restriction area that allows to change the cooling rate over a wide range. Changes in  $K$  value lengthwise of the channels, except mentioned structural parameters, depend on Reynolds number as well. Fig. 4, 5, 6

and 7 show the changes in Reynolds number and respective changes of  $K$  value in model channels with the hole areas of 1 mm (cases 2, 3 and 4).

**Table 2:** Thermal parameters of models studied

Case	$K = Nu/Nu_0$			
	IP	IS	OP	OS
1	1.95	1.95	1.95	1.95
2	2.25	1.80	4.46	3.20
3	1.93	1.64	3.37	2.29
4	1.75	1.59	2.31	2.06
5	2.22	1.94	3.99	3.09
6	2.01	1.84	2.90	2.27
7	2.19	2.05	2.57	2.20
8	2.31	1.80	3.83	2.68
9	2.02	1.65	3.18	2.24
10	1.85	1.60	2.44	1.94

**Table 3:** Hydraulic parameters of models studied

Case	$f/f_0$			
	IP	IS	OP	OS
1	7.03	7.96	8.00	7.84
2	4.82	6.16	7.95	11.70
3	4.73	5.80	9.53	9.88
4	4.67	5.69	7.15	7.93
5	4.56	7.14	8.32	8.32
6	4.75	7.23	7.69	7.95
7	6.22	8.64	7.62	8.40
8	6.71	8.68	12.00	13.14
9	5.74	6.98	9.06	9.83
10	5.69	7.05	7.61	8.39

**Table 4:** Asymmetrical heat transfer rates

Case	$K_{IP}/K_{IC}$	$K_{OP}/K_{OS}$
1	1	1
2	1.25	1.40
3	1.18	1.47
4	1.10	1.12
5	1.15	1.29
6	1.09	1.28
7	1.07	1.17
8	1.28	1.43
9	1.22	1.42
10	1.16	1.26

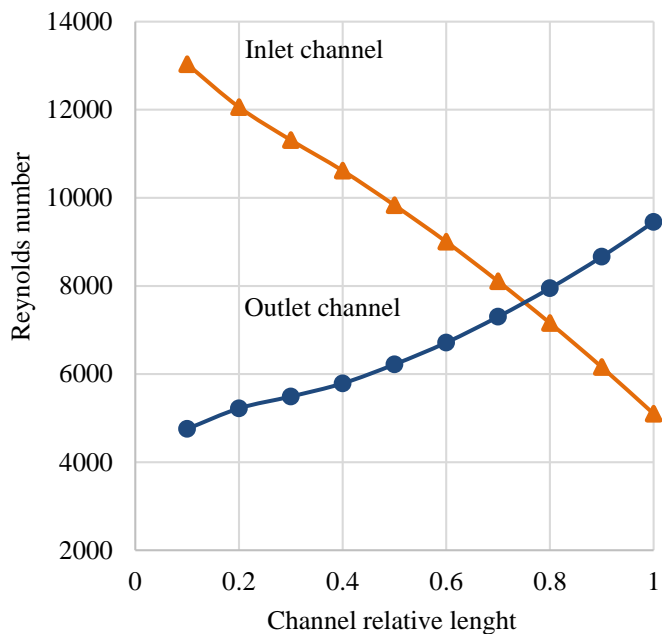


**Figure 4:** Distribution of Reynolds numbers lengthwise of the channels, case 2

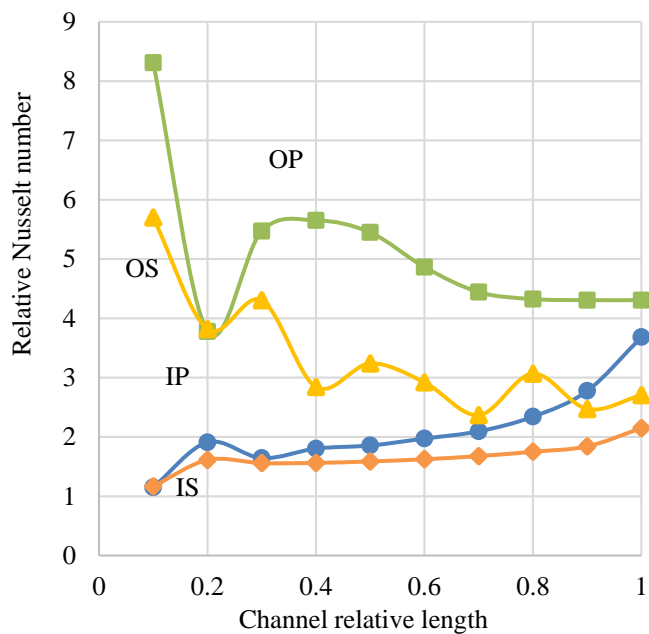


**Figure 5:** Distribution of  $K$  values lengthwise of the channels, case 2

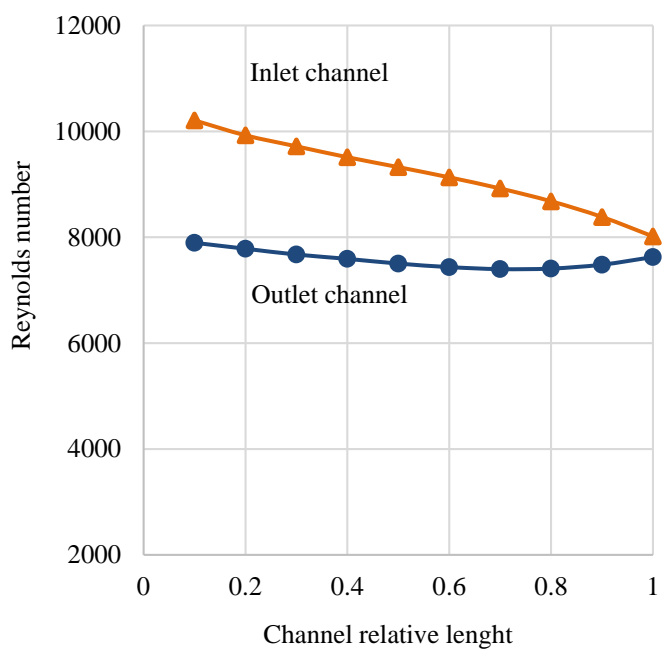


**Figure 6:** Distribution of Reynolds numbers lengthwise of the channels, case 4

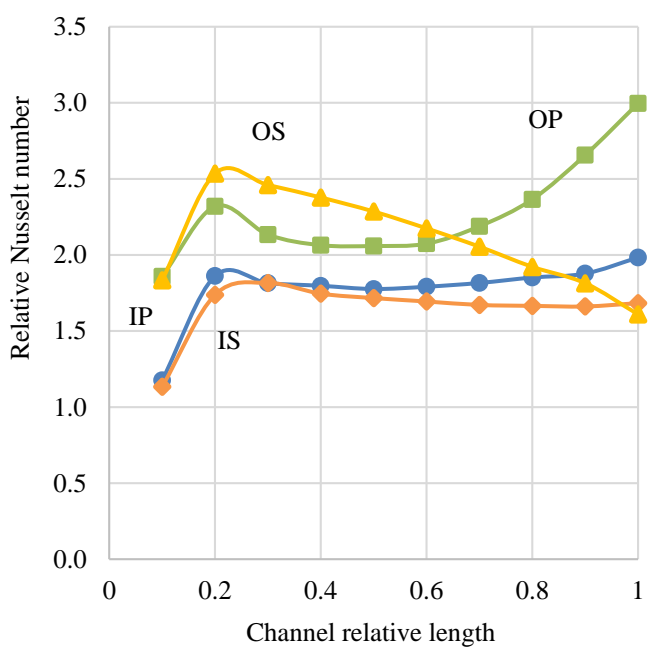


**Figure 7:** Distribution of  $K$  values lengthwise of the channels, case 4

As shown in Fig. 4 and 6, the heat transfer augmentation in the outlet channel is higher than in the inlet channel by 1.5-2.5 times depending on Reynolds number. The channel system forms a complex three-dimensional flow restricting drawing of criterion dependencies for calculation of local heat transfer coefficients considering all geometrical parameters.

Examination of the geometry of each channel with determination of the heat-transfer intensification coefficients is more reasonable.

Visualisation of streamlines (Fig. 8) shows that the proposed channel system operates in the following way.

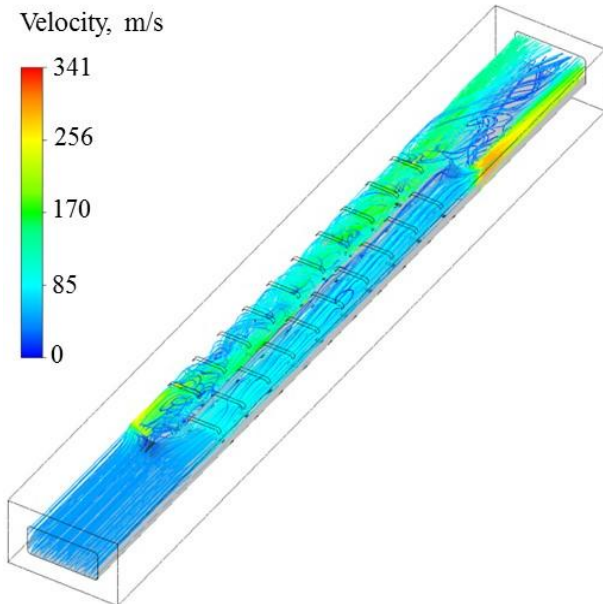


**Figure 8:** Visualisation of streamlines

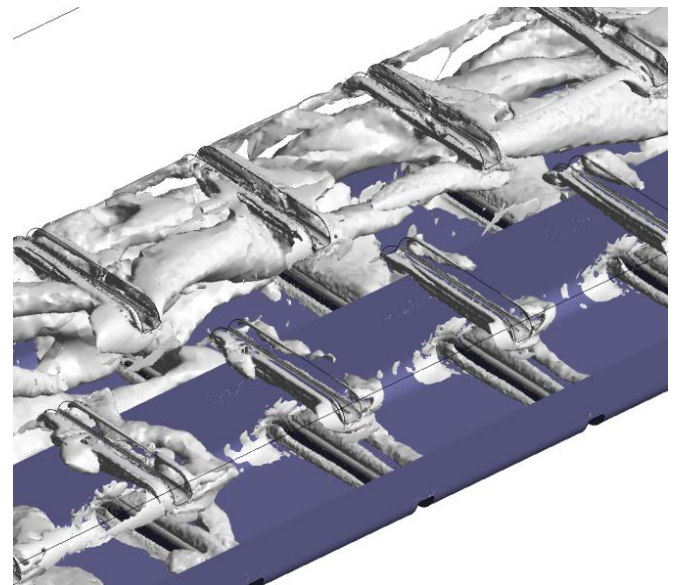


**Figure 9:** Visualisation of vortex structures

The air flows through the inlet channel, decelerates by guiding ribs installed on the pressure side wall and then flows in the outlet channel. The overshadowing ribs in the outlet channel, installed on the pressure side wall, form the detached flow regions in which the air streams pass from the through holes. The air flow through the holes formed by the guiding ribs provides a one-side rundown of the boundary layer on the inlet channel wall from the pressure side, while the overshadowing ribs – one-side jet intensification of the heat transfer on the outlet channel wall from the suction side.

A complex flow pattern makes difficult to obtain the criterion dependencies for calculation of local heat transfer coefficients which might take in to account all geometric parameters of the channels.

Visualisation of vortex structures is shown in Fig. 9. It can be seen that multiple concentrated vortices are formed in the outlet channel as a result of a jet interaction generated by the flow throughout the holes in the separation rib and main cross-flow in the outlet channel.

Examination of a blade with the serpentine-like cooling channel system has been conducted to prove the simulation results. The blade was fabricated using selective laser sintering method. The feather cross section is shown in Fig. 10. Channels K3, K4, K5 and K6 were provided with the proposed intensification system.

Tests were carried out using the calorimetric measurement method in a liquid-metal thermostat [9, 10].

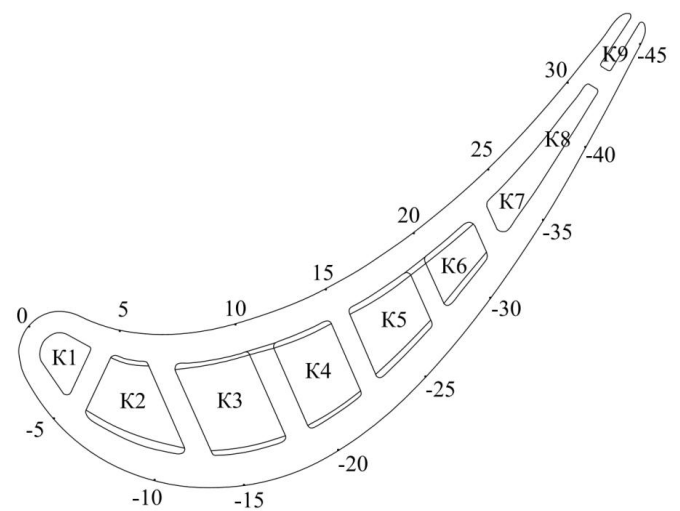


**Figure 10:** Blade cross section, midsection heightwise of the feather

The blade was tested at five different pressure differences.  $P/P_j = 1.49; 1.68; 1.78; 1.97; 2.37$ . Three experiments were performed for each mode. The local coefficients of heat transfer to the cooling air were obtained (Fig. 11). The difference of heat transfer coefficients in the adjacent radial channels were due to a different rate of the heat transfer augmentation and a different value of local temperatures used for calculation of heat transfer coefficients. The heat transfer augmentation in radial channels from the pressure side is higher than from the suction side by 1.8-2.0 times.

### Heat transfer coefficients

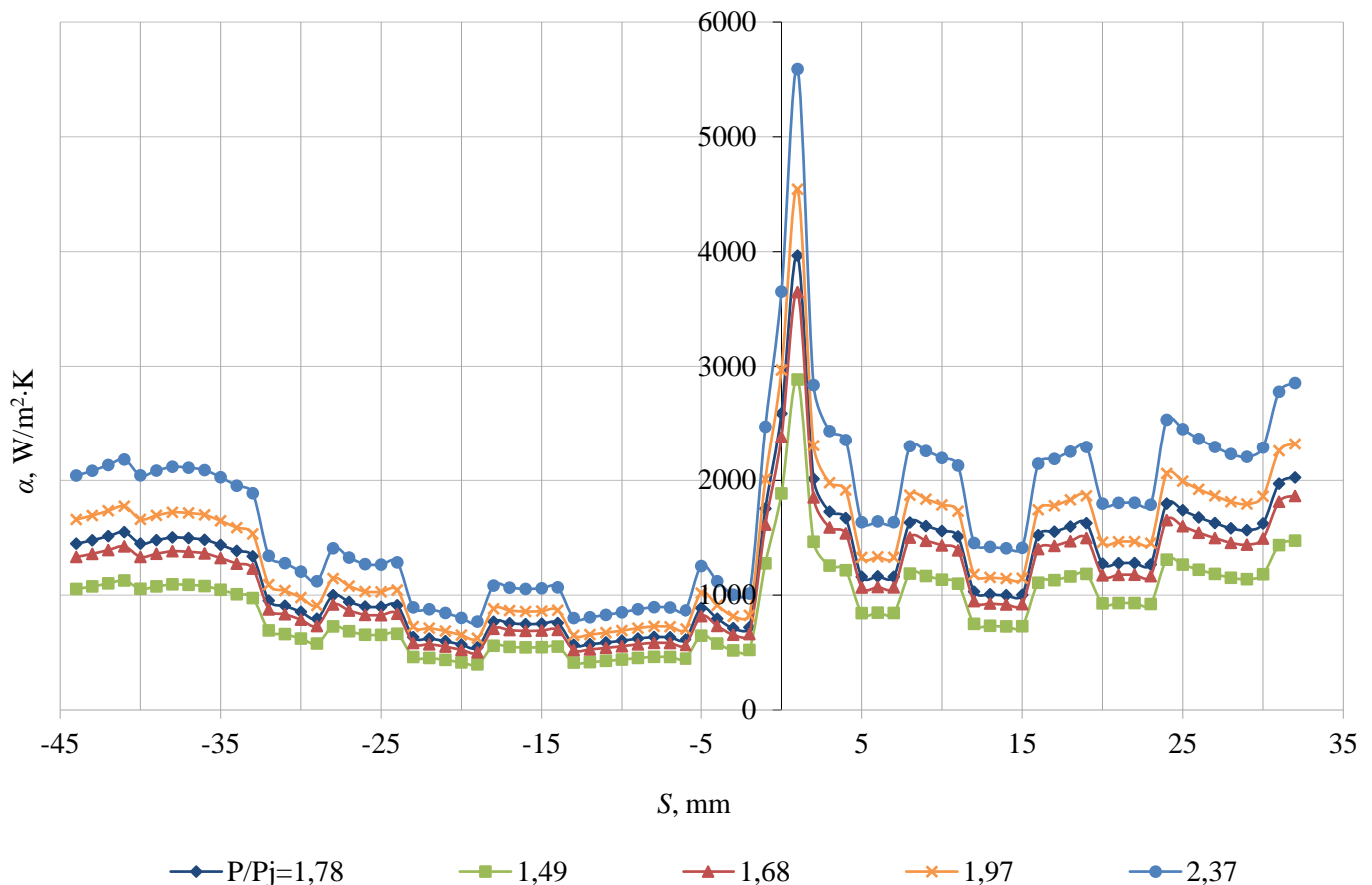


**Figure 11:** Distribution of heat transfer coefficients to the cooling air along the internal surface of the feather midsection depending on a pressure difference

### CONCLUSION

This paper shows that the use of the new asymmetric cooling system will allow to provide a high overall level of heat transfer intensification  $Nu/Nu_0 = 2-3$ .

The best investigated cases provides heat transfer exceeding on the target surface by 30-40%. At the same time, on the opposite surface, the degree of intensification is almost the same as in traditional finned channels. In general, best geometric configuration is case 2.

Experimental with calorimetric measurement method shows that the heat transfer augmentation in radial channels from the pressure side (target side) is higher than from the suction side by 1.8-2.0 times

### ACKNOWLEDGEMENTS

The results were obtained during the implementation of the project of the state task of the Ministry of Education and Science of the Russian Federation in the field of scientific activity No. 13.7616.2017/8.9.

### REFERENCES

- [1] Han, J.-C., Dutta, S., and Ekkad, S., 2012, Gas turbine heat transfer and cooling technology. CRC Press, USA.
- [2] Ito, S., Saeki, H., Inomata, A., et al., 2003, "Conceptual design and cooling blade development of 1700°C – Class high temperature gas turbine", Proc. ASME Turbo Expo, Atlanta, USA.
- [3] Han, J.-C., Zhang, P., 1991, "Effect of rib-angle orientation on local mass transfer distribution in three-pass ribroughened channel", Journal of Turbomachinery, 13, pp. 123-130.
- [4] Han, J.-C., Wright, L. M., 2006, Enhanced internal cooling of turbine blades and vanes. The Gas Turbine Handbook, U.S. Department of Energy, pp. 321-354.
- [5] Hennecke, D. K., Metzger, D. E., and Afgan, N. H., 1984, "Heat transfer problems in aero-engines", Proc. of the International Centre for Heat and Mass Transfer in Rotating Machinery, Dubrovnik, Yugoslavia.

- [6] Glezer, B., Moon, H. K., O'Connell, T. A, 1996, A novel technique for the internal blade cooling, Proc. International Gas Turbine and Aeroengine Congress and Exhibition, Birmingham, UK.
- [7] Zaryankin, A. E., Garanin, I. V., Khudyakova, V. P., Kindra, V. O., and Lisin, E. M., 2016, "CFD investigation of flow in finned plane and conical diffusers", International Journal of Applied Engineering Research, 11(22), pp. 11081-11088.
- [8] Zaryankin, A. E., Garanin, I. V., Grigoriev, E. Y., Kindra, V. O., and Khudyakova, V. P., 2016, "CFD assessment of aerodynamic efficiency improvement methods for steam turbine exhaust hood", International Journal of Applied Engineering Research, 11(21), pp. 10648-10654.
- [9] Shevchenko, I. V., Rogalev, A. N., Shevchenko, M. I., and Vegeera, A. N., 2017, "Method of calorimetric measurements in molten metal thermostat and its application for developing blade cooling system of gas turbines", International Journal of Applied Engineering Research, 12(10), pp. 2382-2386.
- [10] Kopelev, S. Z., Galkin, M. N., Kharin, A. A., and Shevchenko, I. V., 1993, Thermal and hydraulic characteristics of gas turbine blades. Mechanical Engineering, Russian Federation